

Flow injection amperometric sensing of uric acid and ascorbic acid using the self-assembly of heterocyclic thiol on Au electrode

Ramendra Sundar Dey · Susmita Gupta ·
Rupankar Paira · Shen-Ming Chen · C. Retna Raj

Received: 24 June 2010 / Revised: 8 December 2010 / Accepted: 12 January 2011 / Published online: 29 January 2011
© Springer-Verlag 2011

Abstract Au electrode modified with the self-assembled monolayer of a heterocyclic thiol, mercaptotriazole (MTz), is used for the electroanalysis of uric acid (UA) and ascorbic acid (AA). MTz forms a less compact self-assembly on Au electrode. The self-assembly of MTz on Au electrode favors the oxidation of UA and AA at less positive potential. Significant decrease (~400 mV) in the overpotential and enhancement in the peak current for the oxidation of interfering AA with respect to the unmodified electrode is observed. The negative shift in the oxidation peak potential of AA favors electrochemical sensing of UA without any interference. Two well-separated voltammetric peaks for AA and UA are observed in their coexistence. The large separation between the two voltammetric peaks allows the simultaneous or selective sensing of the analytes without compromising the sensitivity. Linear response is obtained for a wide concentration range. This electrode could sense as low as 1 μM of UA in the presence of 10-fold excess of interfering AA. No change in the sensitivity (0.012 $\mu\text{A}/\mu\text{M}$) of the electrode toward UA in the presence and absence of AA is observed. Reproducible and stable amperometric flow injection response was obtained upon repetitive injection.

Keywords Self-assembled monolayer · Mercaptotriazole · Flow injection analysis · Uric acid · Ascorbic acid

Introduction

Uric acid (UA) is a primary end product of purine metabolism. Quantification of UA in serum and urine is of great interest as the elevated levels of UA are symptom of several disease such as gout, hyperuricemia, etc. [1]. Abnormal level of UA leads to kidney damage and cardiovascular disease [2]. Various methodologies have been developed for the precise quantification of UA [3–5]. Enzyme-based colorimetric methods are conventionally used in the clinical laboratories. The electrochemical methods are very promising for the determination of UA, mainly because they are less time-consuming than those based on colorimetric methods. Quantification of UA can be achieved electrochemically by its direct oxidation on solid electrodes or by the enzymatic reaction. The enzyme-based electrochemical methods involve either the (a) use of redox mediator that mediates electron transfer or (b) measurement of enzymatically generated H_2O_2 . Although the enzymatic methods are highly selective and sensitive, they suffer from the lack of long-term operational and storage stability. The direct oxidation of UA on solid electrode requires large overpotential and invites interference due to coexisting easily oxidized biomolecules such as ascorbic acid (AA). Because the concentration of AA is significantly high in the physiological system and the oxidation of AA occurs on the unmodified electrode almost at the same potential as UA, it is a challenging task to measure the concentration of UA in presence of AA. Pretreated and modified electrodes based on carbon nanotubes, metal nanoparticles, molecular self-assemblies, etc. have been

Electronic supplementary material The online version of this article (doi:10.1007/s10008-011-1311-1) contains supplementary material, which is available to authorized users.

R. S. Dey · S. Gupta · R. Paira · C. R. Raj (✉)
Department of Chemistry, Indian Institute of Technology,
Kharagpur 721302, India
e-mail: cretnaraj@yahoo.com

S.-M. Chen
Department of Chemical Engineering and Biotechnology,
National Taipei University of Technology,
No. 1, Section 3, Chung-Hsiao East Road,
Taipei 106 Taiwan, Republic of China

traditionally used for the electroanalysis of UA [4–12]. However, most of these methods require preconcentration and activation of the electrode after each measurement [5]. Surfactant or polymer composite film-modified electrodes are well-known for the sensitive determination of AA and UA [13–15]. Moreover, the enzyme uricase has been widely used in the development of UA biosensors [7, 16–18]. It is desirable to develop cost-effective, sensitive, selective, and stable voltammetric methods for the accurate measurement of UA.

Self-assembling of aliphatic and aromatic thiols is one of the approaches for the modification of Au electrodes. The spontaneous adsorption of thiols and disulfides yield a stable and well-organized monolayer assembly on the coinage electrode surface [19–21]. Aromatic thiols are highly anisotropic in nature and thus enable intermolecular interactions to be stronger than those between alkane thiols. They offer advantages with respect to their structure and chemical reactivity which provide the essential properties for derivatization with multiple chemically specific functional groups and metal complexation [22]. The reduced molecular flexibility of the rings and the π - π stacking interactions between aromatic molecules lead to molecular packing structures and ordering, different from those commonly observed for alkane thiols [23]. Our group is interested in utilizing the self-assemblies of heterocyclic thiols in the development of electrochemical sensors [24, 25]. In continuation of our earlier work, herein we describe the electroanalysis of UA and AA using the self-assembled monolayer (SAM) of mercaptotriazole (MTz) on Au electrode. The analytical performance of the electrode was evaluated by using flow injection amperometric measurement.

Experimental

Chemicals

3-Mercapto-1,2,4-triazole, UA, and AA were obtained from Sigma-Aldrich. All other chemicals used in this investigation were of analytical grade. All the solutions were prepared in deionized water (MilliQ system). Sodium phosphate buffer solution (PBS) of pH 7.2 (0.1 M) was used as supporting electrolyte in all voltammetric measurements. All experiments were carried out under argon atmosphere at room temperature.

Instrumentation

All the voltammetric measurements were performed with CHI643B electrochemical analyzer attached with a Faraday cage/picoampere booster (CH Instruments, Austin, TX, USA). A two-compartment three-electrode cell with a polycrystalline Au working electrode (2 mm diameter, BAS,

USA), a platinum wire auxiliary electrode, and an Ag/AgCl (3 M KCl) reference electrode was used in the measurements. The following optimized instrumental parameters were used for square-wave voltammetric (SWV) measurements. Square-wave amplitude is 25 mV, frequency is 15 Hz, step potential is 4 mV, and quiet time is 2 s. The flow injection analysis experiments were carried out with a CHI842B dual channel electrochemical detector (CH Instrument, Austin, TX, USA). The flow rate of the mobile phase (PBS of pH 7.2) was controlled by BAS LC peristaltic pump (PM-80) with Teflon tubing. An electrochemical cell with Ag/AgCl (3 M NaCl) and stainless steel auxiliary and dual Au working electrode (3 mm diameter) were used in the flow injection experiments. Thickness of the Teflon gasket was 0.002 in. The sample was delivered to the electrochemical cell at the flow rate of 1 ml/min from a reservoir.

Electrode modification

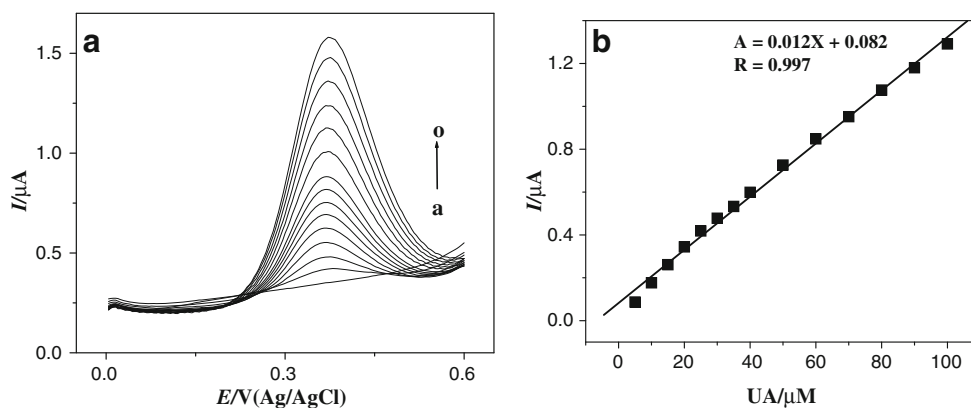
Polycrystalline Au electrodes were polished well with alumina powder (0.06 μm) and sonicated repeatedly in water for 5–10 min. The polished electrodes were then electrochemically cleaned by cycling the potential between -0.2 and 1.5 V at the scan rate of 10 V/s in 0.25 M H_2SO_4 until the characteristic cyclic voltammogram for a clean Au electrode was obtained. The pretreated electrode was then immersed in an aqueous solution of MTz (1 mM) for a required period of time (2 h) at room temperature for the formation of SAM. Hereafter the Au electrode modified with the monolayer of MTz will be denoted as Au-MTz. This SAM-modified electrode was washed extensively with deionized water to remove the physically adsorbed thiol and subjected to voltammetric experiments. The real surface area of the Au electrode was obtained from the charge consumed during the reduction of surface oxide, and area was calculated to be 0.077 cm^2 . The real surface area was used in the calculation of capacitance, surface coverage (Γ) of the monolayer, and sensitivity of the electrode toward analytes.

Results and discussion

Electrochemical characterization of Au-MTz electrode

The self-assembly of MTz was electrochemically characterized by measuring the capacitance and surface coverage (Γ). The capacitance of the monolayer was obtained at 0 V, using the non-Faradic current [26], and was 28 ± 2 $\mu\text{F cm}^{-2}$. The Γ of the MTz monolayer was obtained from the charge consumed during its reductive desorption in 0.1 M KOH. Au-MTz shows multiple desorption peaks in the potential range -0.58 to -1 V which is similar to those obtained for other

Fig. 1 (a) Square-wave voltammograms obtained for the sensing of UA on Au-MTz electrode in 0.1 M PBS (pH 7.2). [UA]: (a) 0, (b) 5, (c) 10, (d) 15, (e) 20, (f) 25, (g) 30, (h) 35, (i) 40, (j) 50, (k) 60, (l) 70, (m) 80, (n) 90, and (o) 100 μM . (b) Corresponding calibration plot. (please add the full stop).

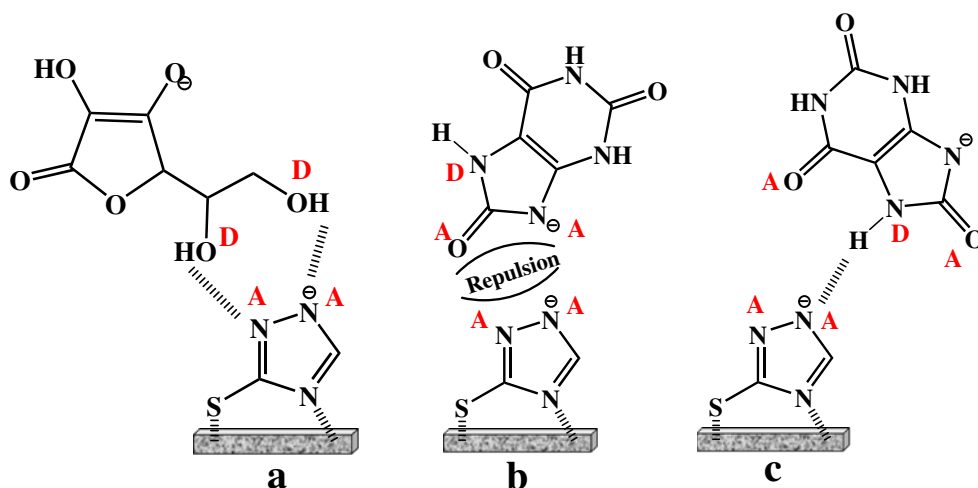


heterocyclic SAMs having perpendicular orientation on Au surface [27, 28]. The multiple voltammetric peaks obtained during the reductive desorption is due to the heterogeneity of the electrode surface. The peaks can be ascribed to the molecules adsorbed at different facets of the polycrystalline Au. It is known that reductive desorption of SAM on different low index faces of Au occurs apparently at different potentials [27]. It is considered that the MTz adopts near-perpendicular orientation on electrode surface. The Γ value was determined from the charge consumed during desorption of the monolayer and was $2.94 \pm 0.06 \times 10^{-10} \text{ mol cm}^{-2}$. The capacitance and Γ values are very close to those obtained for mercaptoprimidine-based monolayers on Au electrode [24]. The cyclic voltammograms obtained for $\text{Fe}(\text{CN})_6^{3-/4-}$ redox couple on MTz electrode is very similar to those obtained on an unmodified Au electrode (Supplementary information), indicating the free diffusion of redox molecule to the electrode. The compact monolayers are known to inhibit the free diffusion of redox molecules. In the present case, the monolayer on the electrode surface does not impede the diffusion of redox molecule, suggesting that the MTz monolayer is not very compact.

Electrochemical oxidation of UA and AA

Electrochemical oxidation of UA involves two electrons and is dependent on solution pH. On unmodified Au electrode, UA oxidation occurs at $\sim 0.45 \text{ V}$ in the first potential sweep. The peak potential shifts to more positive potential, and the peak current gradually decreases in the subsequent sweeps, presumably due to the deactivation of electrode surface by the oxidation product. On the other hand, stable and well-defined voltammograms were obtained on the MTz monolayer-modified electrode (Supplementary information), though the peak potential is close to that of the unmodified electrode. Unlike the polycrystalline Au electrode, the peak current and peak potential did not change upon repeated sweeps, indicating that the electrode does not undergo deactivation during oxidation process. The oxidation peak current linearly scales with the square root of scan rate (Supplementary information), indicating that the oxidation process is diffusion-controlled. Figure 1 shows the SWVs obtained for UA on the MTz monolayer-modified electrode in the micromolar range. The SWV peak at 0.37 V increases linearly with increase in the concentration of

Fig. 2 Schematic illustration of possible hydrogen-bonding interaction of AA (a) and UA (b, c) with the MTz monolayer. A and D represents acceptor and Donor.



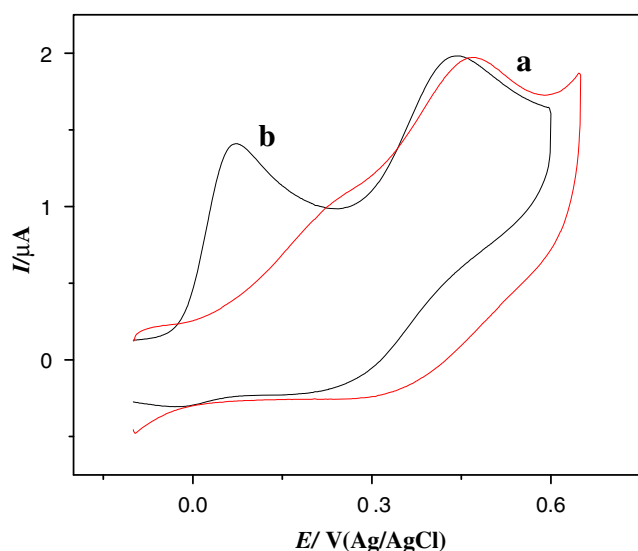


Fig. 3 Cyclic voltammograms obtained for AA and UA in their coexistence on (a) unmodified Au and (b) Au-MTz electrodes. Scan rate, 50 mV/s.

UA. The calibration plot is linear in the concentration range 1–100 μM , and the sensitivity was found to be $0.172 \pm 0.011 \mu\text{A cm}^{-2} \mu\text{M}^{-1}$. The limit of detection (3σ) of UA on Au-MTz electrode by SWV is 1 μM .

AA is known to be a major interfering agent in the voltammetric sensing of UA. Oxidation of UA and AA on unmodified electrodes occurs almost at the same potential. The unmodified Au electrode shows a broad voltammetric peak at ~ 0.45 V. The voltammetric response on the unmodified Au electrode is not stable, the oxidation peak shifts to more positive potential, and the peak current decreases in the subsequent sweeps. The unstable behavior is presumably due to the fouling of electrode surface. However, a well-defined voltammetric peak was obtained at ~ 0.075 V on Au-MTz electrode (Supplementary information). A 400-mV decrease in overpotential with respect to the unmodified Au electrode was observed without using any redox mediator. The monolayer assembly prevents fouling of

the electrode surface and facilitates the oxidation of AA. The specific interaction between triazole moiety on the electrode surface and AA is expected to play an important role in decreasing overpotential. The voltammetric response is reproducible and highly stable. The sharp and well-defined peak reflects the fast electron transfer kinetics on the electrode surface. It should be pointed out here that although both AA and UA have similar diffusion coefficient (6.53×10^{-10} and $6.6 \times 10^{-10} \text{ m}^2/\text{s}$, respectively) [29] and are negatively charged (the $\text{p}K_{\text{a}}$ of UA and AA are 5.8 and 4.16, respectively) at the experimental condition used, the Au-MTz electrode could successfully distinguish their voltammetric peaks. Moreover, the surface $\text{p}K_{\text{a}}$ of MTz is reported to be 4.9 [30], and hence, it is expected to be partially or fully ionized at neutral pH. One would expect an electrostatic repulsion of anionic analytes at the monolayer of MTz. However, as shown in Fig. 2, the molecular structure of AA favors a strong double hydrogen-bonding interaction with MTz. Such double hydrogen-bonding interaction is not favorable for UA. The strong hydrogen-bonding interaction AA with the monolayer is believed to play a vital role in the facilitated oxidation of AA. Furthermore, as the formal potential of AA is more negative than the potential at which the oxidation actually occurs at unmodified electrode [31], it is reasonable to expect the negative shift of the oxidation potential for AA.

Simultaneous electroanalysis of UA and AA

Because the concentration of AA in the physiological system is significantly high, it is a challenging task to quantify the concentration of UA in the presence of AA. The unmodified electrode could not show separate voltammetric peaks for UA and AA in their coexistence. A broad voltammetric peak at the potential of 0.45 V was observed for both the analytes. The voltammetric response was not stable in the subsequent sweeps, indicating the gradual deterioration of the electrode surface. However, two well-separated voltammetric peaks

Table 1 Oxidation of AA and UA on the different aromatic and heteroaromatic monolayer-modified electrodes.

Electrodes	Oxidation potential E_{p}/V (vs. Ag/AgCl)		Peak separation (V)	LOD for UA (μM)	Reference
	AA	UA			
Au/MBI	0.08	0.34	0.28	1	[31]
Au/MQ	0.61	0.62	0.01	–	[32]
Au/TA	0.24	–	–	–	[33]
GC/DHB	0.10	0.32	0.22	–	[34]
GC/ <i>o</i> -AP	0.26	0.60	0.34	14	[35]
WGE/Qu	0.02	0.30	0.28	1	[36]
Au/MTz	0.02	0.36	0.34	1	This work

MBI: mercaptobenzimidazole, MQ: 8-mercaptoquinoline, TA: 3-amino-5-mercapto-1,2,4-triazole, DHB: 3,4-dihydroxybenzaldehyde, *o*-AP: *o*-aminophenol, Qu: quercetin

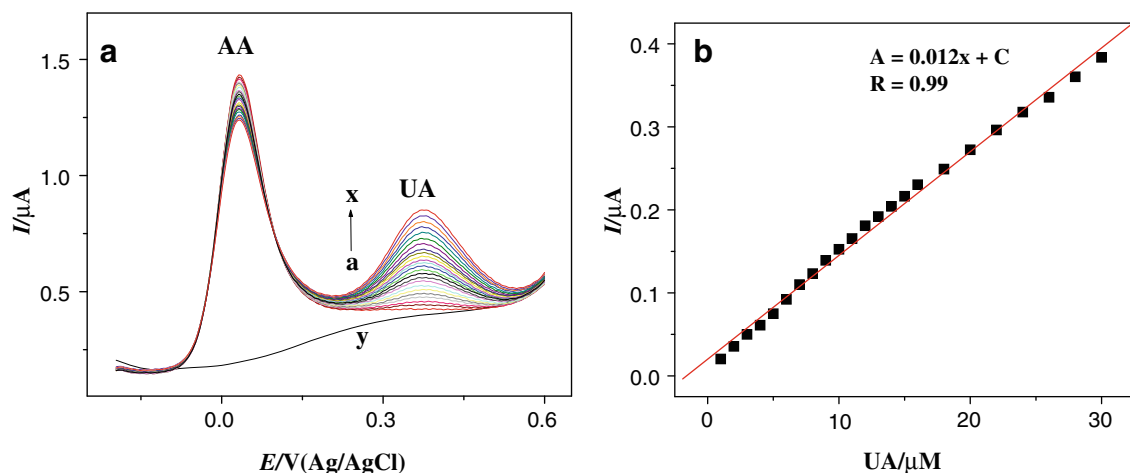


Fig. 4 (a) Square-wave voltammograms obtained for the sensing of UA in the presence of large excess of AA (100 μM) in 0.1 M PBS (pH 7.2). [UA]: (a) 0, (b) 1, (c) 2, (d) 3, (e) 4, (f) 5, (g) 6, (h) 7, (i) 8, (j) 9, (k) 10, (l) 11, (m) 12, (n) 13, (o) 14, (p) 15, (q) 16, (r) 18, (s) 20, (t) 22, (u) 24, (v) 26, (w) 28, and (x) 30 μM . (y) Square-wave voltammetric response of Au-MTZ in the absence of AA and UA. (b) Corresponding calibration plot for UA.

were obtained on the MTz monolayer-modified electrode (Fig. 3). The separation between the two voltammetric peaks was estimated to be 340 mV, which is significantly higher than those reported in the literature on the monolayer-modified electrodes (Table 1) [31–36]. Voltammetric response on the modified electrode is highly stable; the peak potential and peak current did not change in the subsequent sweeps. Figure 4 displays the voltammetric response of MTz electrode toward UA in the presence of fixed concentration of AA. Gradual increase in the voltammetric peak corresponding to UA was obtained. The sensitivity of the electrode in the presence of 10-fold excess of AA was 0.012 $\mu\text{A}/\mu\text{M}$, which is very same as that obtained in the absence of AA (Fig. 1). It confirms that the coexistence of AA does not influence the sensing capability of the MTz monolayer-modified electrode. The analytical performance of the modified electrode was

further tested by simultaneously changing the concentration both the analytes. Gradual increase in the voltammetric peak current with concentration was noticed (Supplementary information). The performance of the MTz-modified electrode is excellent with respect to the existing other monolayer-modified electrodes (Table 1).

Flow injection amperometric response of the electrode was obtained to further evaluate the performance of the electrode (Fig. 5). The electrode potential was held at 0.07 and 0.45 V for AA and UA, respectively, and aliquots of the analytes were injected. As can be seen, stable and reproducible response was obtained during the repeated injection of the analytes. The relative standard deviation in the amperometric current was calculated to be 7.5% and 4.7% for UA and AA, respectively. The amperometric response obtained confirms that the electrode is highly stable and can be used for repeated measurements.

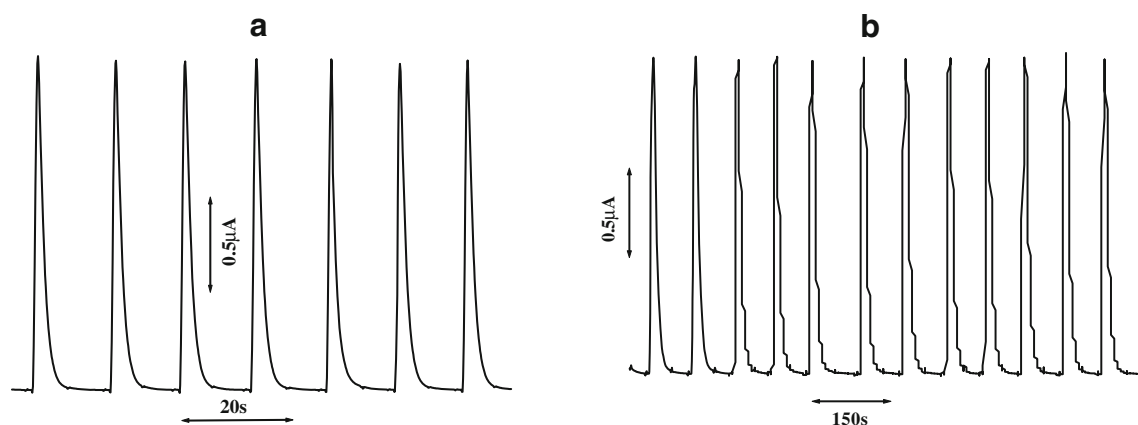


Fig. 5 Flow injection responses obtained by repetitive injection of 50 μM (a) UA and (b) AA at an applied potential of 0.45 and 0.07 V, respectively, on Au-MTZ electrode in 0.1 M PBS (pH 7.2) as a mobile phase. Flow rate, 1 ml/min.

Conclusions

In conclusion, the simultaneous electroanalysis of UA and AA has been achieved using the heteroaromatic monolayer-modified electrode. The voltammetric peaks are well separated and the simultaneous or selective detection of the analytes is feasible with the monolayer-modified electrode. The favorable interaction of AA with the monolayer assembly on the electrode surface shifts its oxidation potential to less positive potential. The coexistence of AA does not affect the sensitivity of the electrode toward UA. Flow injection amperometric response indicates that the monolayer-modified electrode is robust and can be used for repeated measurements. The electrodes modified with the self-assembly of heterocyclic thiols can be used for the electroanalysis of biologically important analytes.

Acknowledgments This work was supported by Department of Science and Technology (DST) and Indian Institute of Technology, Kharagpur. R.S.D. thanks UGC for research fellowship.

References

1. Drisko JA, Chapman J, Hunter VJ (2003) *J Am Coll Nutr* 22:118–123
2. Simoni RE, Ferreira LNL, Scalco FB, Oliveira CPH, Aquino FR, Oliveira MLC (2007) *J Inher Metab Dis* 30:295–309
3. Cossu A, Orru S, Jacomelli G, Carcassi C, Contu L, Sestini S, Corradi MR, Pompucci G, Carcassi A, Micheli V (2006) *Biophys Acta* 1762:29–33
4. Zen J-M, Chen P-J (1997) *Anal Chem* 69:5087–5093
5. Zhang J, Oyama M (2007) *Electrochem Commun* 9:459
6. Cui Y, Yang C, Pu W, Oyama M, Zhang J (2010) *Anal Lett* 43:22–33
7. Gilmartin MAT, Hart JP (1994) *Analyst* 119:833–840
8. Khoo SB, Chen F (2010) *Anal Chem* 74:5734–5741
9. Zhang Y, Wen G, Zhou Y, Shuang S, Dong C, Choi MMF (2007) *Biosens Bioelectron* 22:1791–1797
10. Wei Y, Li M, Jiao S, Huang Q, Wang G, Fang B (2006) *Electrochim Acta* 52:766–772
11. Privett BJ, Shin JH, Schoenfisch MH (2010) *Anal Chem* 82:4723–4741
12. Shahrokhian S, Khafaji M (2010) *Electrochim Acta* 55:9090–9096
13. Cao X, Xu Y, Luo L, Ding Y, Zhang Y (2010) *J Solid State Electrochem* 14:829–834
14. Cao X, Luo L, Ding Y, Yu D, Gao Y, Meng Y (2009) *J Appl Electrochem* 39:1603–1608
15. Wu S, Wang T, Gao Z, Xu H, Zhou B, Wang C (2008) *Biosens Bioelectron* 23:1776–1780
16. Chen D, Wang Q, Jin J, Wu P, Wang H, Yu S, Zhang H, Cai C (2010) *Anal Chem* 82:2448–2455
17. Behera S, Raj CR (2007) *Biosens Bioelectron* 23:556–561
18. Miland E, Ordieres AJM, Blanco PT, Smyth MR, Fagain CO (1996) *Talanta* 43:785–796
19. Ulman A (1991) *An introduction to ultra thin organic films: from Langmuir–Blodgett to self-assembly*. Academic, Boston
20. Mandler D, Turyan I (1996) *Electroanalysis* 8:207–213
21. Finklea HO (1996) *Electrochemistry of organized monolayers of thiols and related molecules on electrodes*. In: Bard AJ, Rubinstein I (eds) *Electroanalytical chemistry*, vol 19. Marcel Dekker, New York, pp 109–335
22. Jin Q, Rodriguez JA, Li CZ, Darici Y, Tao NJ (1999) *Surf Sci* 425:101–111
23. Whelan CM, Smyth MR, Barnes CJ (1998) *J Electroanal Chem* 441:109–129
24. Raj CR, Behera S (2007) *Langmuir* 23:1600–1607
25. Behera S, Sampath S, Raj CR (2008) *J Phys Chem C* 112:3734–3740
26. Bard AJ, Faulkner LR (2000) *Electrochemical methods—fundamentals and applications*. Wiley, New York
27. Gao Z, Siow KS, Ng A, Zhang Y (1997) *Anal Chim Acta* 343:49–57
28. Madueno R, Sevilla JM, Pineda T, Roman AJ, Blazquez M (2001) *J Electroanal Chem* 506:92–98
29. Ernst H, Knoll M (2001) *Anal Chim Acta* 449:129–134
30. Dey RS, Gupta S, Paira R, Raj CR (2010) *ACS Appl Mater Interfaces* 2:1355–1360
31. Raj CR, Ohsaka T (2003) *J Electroanal Chem* 540:69–77
32. Yang Y, Khoo SB (2004) *Sens Actuators B Chem* 97:221–230
33. Sun Y-X, Wang S-F, Zhang X-H, Huang Y-F (2006) *Sens Actuators B Chem* 113:156–161
34. Arihara K, Ariga T, Takashima N, Okajima T, Kitamura F, Tokuda K, Ohsaka T (2003) *Phys Chem Chem Phys* 5:3758–3761
35. Nassef HM, Radi AE, O’Sullivan C (2007) *Anal Chim Acta* 583:182–189
36. He J-B, Jin G-P, Chen Q-Z, Wang Y (2007) *Anal Chim Acta* 585:337–343